The Electrical Properties of Interfacial Double Layers

A thesis

submitted in partial fulfilment

of the requirements for the Degree

of

Doctor of Philosophy

at the

University of Waikato

by

Mark Hedley Jones

THE UNIVERSITY OF
WAIKATO
Te Whare Wānanga o Waikato

University of Waikato
2011

Abstract

When a solid comes in contact with a liquid, an interfacial double-layer is likely to form. They are too small to feel or see so their presence goes mostly unnoticed at the macroscopic level. Double layers stabilise some of our most important fluids – blood, milk, paints, and inks. Without the protection of double-layers, these mixtures clump and lose their fluidity.

 This thesis looks at both electricity generation and the electrical impedance of interfacial double layers. 

This thesis is separated into two parts, both linked to the behaviour of double-layers. In **??** these layers are used as a means of converting fluid-mechanical energy into electrical energy. The primary application of such a harvester would be to power electronic water meters. Domestic water meters are typically installed where electrical connection is not feasible; harvesting energy here may makes electronic metering more feasible long-term. My findings show that double layer based energy harvesters are not efficient enough for this application yet. Recent literature on the subject suggests large gains in efficiency may be possible using more exotic materials.

Part I models the electrical impedance of submerged electrodes. Double-layers play a large part in determining the electrical impedance between metal-fluid interfaces. This work is important to designers of medical implants; and by extension, anybody who relies on the implants themselves. Engineers use solutions of saline to mimic the environment experienced by their implants once implanted. This gives them a way to test the implant without injuring anyone. A way of characterising the interface between electrodes in solution is to model it mathematically. Such a model was created by my supervisor, Jonathan Scott. I use that model to compare electrodes placed in solutions of saline to those placed in a living animal. Measurements of the two show they are quite different from one another. I create a mixture using low-cost ingredients that closely resembles the electrical impedance of a live animal.

Acknowledgement

Thanks to Jonathan Scott (my chief supervisor), Steve Newcombe (Waikato University's award winning glass blower) and Peter Single (the senior electrical engineer at Saluda Medical) for their time, resources and patience. Thank you to my second supervisor, Marcus Wilson, for checking up every so often and help proof-reading. Thanks also go to the University of Waikato for a funding the first three years of this work with a Waikato Doctoral Scholarship. Without this funding I could not have undertaken this research. The support of my partner, Sarah, and my mother, Gina, has kept me on track. Lastly, thank you to everyone who has contributed to open-source projects, especially those part of:

- The Linux kernel and GNU tools
- Gnome desktop environment
- Inkscape vector drawing software
- Gimp image manipulation program
- The Arch Linux distribution
- TEX and its derivative LATEX
- Python
- ngSpice

Work done throughout this thesis has relied heavily on these tools.

Contents

List of Figures

List of Tables

Part I

Double Layers on Conductors: Electrical Impedance

For the engineers of medical implant devices, knowing the electrical impedance between electrodes is important. Having a tool to simulate such impedances allows those designers to ensure fault free operation of potentially lethal devices. A model of the interface impedance between electrode and electrolyte is presented in the proceeding chapter. That model was created by my chief supervisor Jonathan Scott and Peter Single of Saluda Medical Sydney. Validation of the model was made in a standard solution of saline, but details of how saline concentration affected the parameters were unknown. In part I of thesis thesis I take that model and extend its predictive capability to a range of salinities. Having such a model allows for easy comparison between different electrolytes and electrode geometries. Using that ability, I characterise the interface in an anaesthetised sheep's spinal cavity and compare the results to the various saline solutions measured in the lab. That comparison showed that the situation in live sheep is relatively different to that of standard saline solutions. Using the measurement methods developed, I then find a mixture that closely matches the electrical impedance seen in sheep. This mixture now serves as an improved test solution for the engineers of medical implant devices.

Chapter 1

An Interfacial Model In The Electrical Domain

The work throughout the remainder of this thesis is based upon an interface model put forward by my supervisor and a colleague of his, Peter Single. The model was verified in a single, known concentration of phosphate buffered saline (PBS) at the point I began using it. Working through the processes taken by my supervisor to create his model, I re-created the model from my own measurements. By creating a range of solutions of PBS to test against, I fitted parameters of the initial model to the concentration of PBS. This put me in a good position to compare those solutions to live biological solutions. That comparison is the main scientific contribution resulting from this work.

1.1 The Scott-Single Interface Model

Jonathan Scott and Peter Single recently published an electrical model of an implantable electrode array in saline in 2013 [5]. The intention of that model was to simulate the electrical impedance that a medical implant device would see once implanted into a human spinal cavity. It is also general

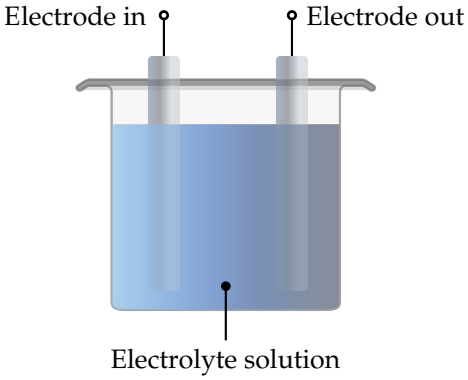

Figure 1.1: Electrodes submerged in an electrolyte solution, such a system can be described by the Scott-Single Interface Model.

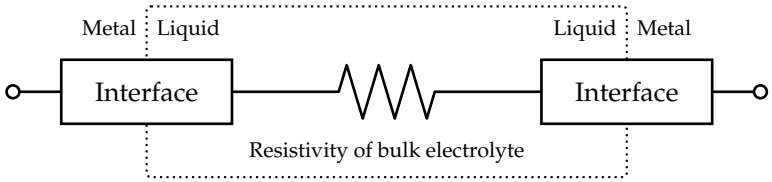

Figure 1.2: Connection diagram of two electrodes (with their interface models) connected together by the resistivity of an electrolyte solution.

enough to use in any situation where electrodes are placed in an electrolyte solution, such as depicted in fig. 1.1.

The model comes in two parts, the electrode interface, and the resistivity of the electrolyte's bulk. Figure 1.2 shows the general electrical configuration of such an electrode-electrolyte system. It shows that there are two interfaces per system, and that the liquid side of those two interfaces are joined electrically by the resistance of the electrolyte's bulk resistivity. The metal side of the interfaces is what the rest of the circuit would connect to. First, the interface model will be explained.

1.1.1 The interface model

The full interface model is represented schematically by fig. 1.3. It represents the transition between the metal of the electrode and the liquid of the

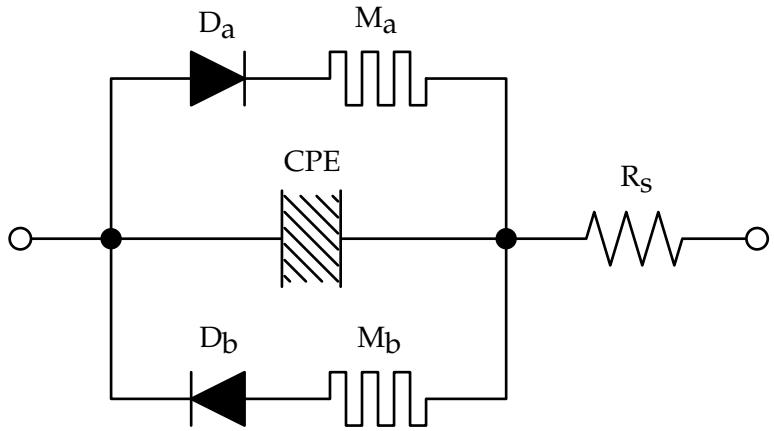

Figure 1.3: Electrical schematic of the electrode-electrolyte interface

electrolyte. The model used throughout this thesis is a slightly simplified version of fig. 1.3 in that the memristors have been removed.

1.1.1.1 Interface series resistance: Resistor

The series resistor at the right hand side of the model schematic (labelled R_S) represents the purely resistive component of the interface's impedance. As it is series with all other components in the interface model, there is no way for charge to cross the interface without encountering this resistance. The parameter used to denote the interface's series resistance is:

- R_S – The series resistance of the interface

1.1.1.2 Polar effects: Constant phase element

At the centre of the model is the constant phase element, or CPE. A CPE, or fractional pole capacitor, is a device that behaves like a cross between a capacitor and a resistor. They are primarily used to describe the capacitance of double layer interfaces, the function it serves in this model. It is capacitive in the sense that voltage leads current, but by an amount less than 90°. Mathematically, the 90° angle between sinusoidal voltages and currents in a

capacitor is a result of the capacitors current being $I(t) = C \times \frac{dV(t)}{dt}$. When $V(t)$ is a sine wave, this becomes $I(t) = C \times \frac{dSin(t)}{dt}$, which is the same as $I(t) = C \times Cos(t)$. The angle between Sine and Cosine is always 90, and this is why a capacitors impedance is $-90°$ out of phase. A CPE, on the other hand, has a phase angle somewhere *between* 0 and $-90°$. This requires a fractional differentiation of $I(t) = C \times \frac{dV(t)}{dt}$, something uncommon outside of pure mathematics. A consequence of having a current/voltage relationship of less than 90°, a CPE'S impedance magnitude decays at a rate lower than $20\frac{dB}{decade}$.

SPICE, or any other commonly used circuit simulators, does not support fractional pole capacitors so entering one into the model will require building it up from discrete components. In 1959, Morrison demonstrated a

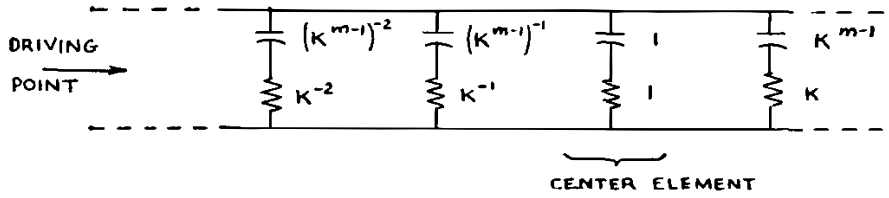

Figure 1.4: Ralph Morrison's implementation of a constant phase element using an infinite array of resistor-capacitor pairs (taken from Morrison's paper – [4]).

way of creating constant phase elements from an infinite array of resistor-capacitor (RC) pairs [4]. One of Morrison's implementations of a constant phase element is presented as fig. 1.4. Each parallel branch has precisely chosen resistor and capacitor values such that when summed together the impedance magnitude versus frequency is a constant slope, i.e., the impedance does not flatten at a particular frequency as it would with a single RC pair. Creating any element comprised of an infinite number of sub-elements is not possible, but by selecting only those elements that contribute to the bandwidth of interest the result is the same within the selected

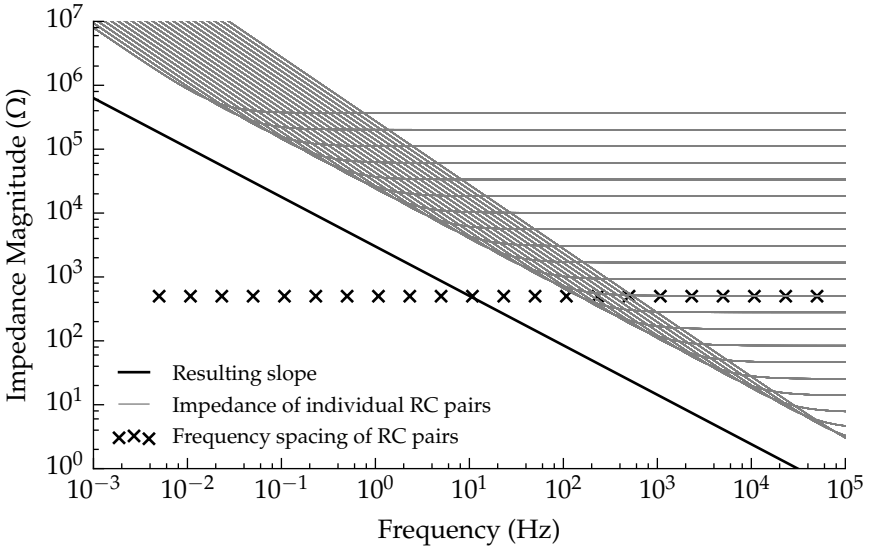

Figure 1.5: Graph showing how a non 20 dB per frequency decade

frequency window. Using that method and selecting only RC pairs with a cut-off frequency in the range of 1 mHz to 1 MHz, a practical CPE element is created.

Figure 1.5 shows the individual contributions from each RC branch in an implementation of a CPE. Each of grey trace represents a single RC branch in the CPE element, each displaying a high-pass filter slope. The value of the resistor in each branch is evident by the vertical spacing of the traces, clearly visible to the right of the graph. The branches in this particular example have been spaced in the frequency domain at a density of three per decade, as shown by the black crosses. This means that per decade of frequency, there are three corner frequencies, each relating to an RC pair. Because each of there branches are in parallel the total response of the CPE is the sum of each branch, that response is shown as the black trace on the graph. The critical observation is that the slope of the resulting trace is not the same as each of the individual branches. This allows the CPE to behave

fractionally as a capacitor, being anywhere between resistive (flat response) and capacitive (20 dB/decade slope).

The CPE is represents readily reversible reactions, polar reorientation, and ionic repulsion and attraction between the electrode surface and electrolyte. It is capacitive in nature because each of these mechanisms store charge, which can be drawn back by reversing the applied electromotive force. Parameters used to describe the behaviour of the CPE are:

- m – Slope of the CPE's frequency response
- k – Spacing, or density, of R-C branches with frequency
- $|Z|$ @ 1 kHz – Sets the vertical position of the magnitude of CPE's frequency response at a known frequency

1.1.1.3 Faradaic reactions: diodes

If the voltage placed across the interface is kept within certain limits, the CPE and series resistance (R_S) would be all that is necessary to accurately mimic a single electrode-electrolyte interface. But once the electric potential across the interface becomes high enough, Faradaic reactions will occur at the electrode's surface. Faradaic reactions are reactions involving charge transfer, adding ionised species to the electrolyte and often producing gas. Gas, or any new species, is bad news in an implanted setting as this causes damage to the patient. Possible faradaic reactions between saline and plat-

inum electrodes are:

$$Pt + H_2O \Leftrightarrow PtO + 2H^+ + 2e^- \tag{1.1}$$

$$PtO + H_2O \Leftrightarrow PtO_2 + 2H^+ + 2e^- \tag{1.2}$$

$$Pt + H^+ \Leftrightarrow Pt - H \tag{1.3}$$

$$Pt + H_2O + e^- \Leftrightarrow Pt - H + OH^- \tag{1.4}$$

The electrical current density through an electrode as a function of electrode overpotential and the cathodic and anodic reactions occurring at each electrode is given by:

$$i_{net} = i_0 \left\{ \frac{[O]_{(0,t)}}{[O]_\infty} e^{-\alpha_c n f \eta} - \frac{[R]_{(0,t)}}{[R]_\infty} e^{(1-\alpha_c) n f \eta} \right\} \tag{1.5}$$

This is the current-overpotential equation and is derived from the more general Butler-Volmer equation [3, 5]. In eq. (1.5), i_{net} is the net Faradaic current across the electrode/electrolyte interface, i_0 is the exchange current density, $[O]_{(0,t)}$ and $[R]_{(0,t)}$ are the concentrations at the electrode surface as a function of time, $[O]_\infty$ and $[R]_\infty$ are concentrations of reactant in the bulk electrolyte, α_c is the cathodic transfer coefficient (approximately 0.5), n is the number of moles of electrons per mole of reactant oxidised, f is Faraday's constant divided by the the product of the gas constant and the absolute temperature (F/RT), and η is the electrode overpotential. This equation describes the forward and reverse electrical current through an electrode by separating the forward and reverse reactions; oxidisation and reduction.

$$I = i_0 e^{V_D / n V_T} \tag{1.6}$$

Taking a single half of the equation, either the reduction or oxidisation,

yields an equation that is similar to that of a diode; an observation made by McAdams and utilised in the Scott-Single model [2]. The standard diode equation is shown as eq. (1.6), where I is the current through the diode, i_0 is the diode saturation current, V_D is the potential across the diode, n is the diode's ideality factor, V_T is the thermal voltage (defined as the product of Boltzmann's constant and temperature divided by the charge on an electron). The parameters used to describe the behaviour of the diode are:

- i_0 – the diode's saturation current
- n – the diode's ideality factor

The diodes themselves can not account for the relative abundance of reactants for the redox reactions, this must be taken care of separately.

1.1.1.4 Species depletion: memristors

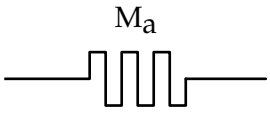

Figure 1.6: Electrical symbol of a memristor, as is used in the original electrode-electrolyte interface model

A memristor is a two port device that sets its resistance based on its own history. Its resistance can either depend on the integral over time of the voltage placed across it or the total charge passed through the device [1]. Its name is a portmanteau of the word 'memory' and 'resistor' owing to its use of memory to set its resistance.

The memristive device models species depletion in the electrolyte by pinching off a diode branch with the amount of current passed through the diode. As the specific Faradaic reaction proceeds, it consumes the reactants from the electrolyte bulk until eventually there is none left. Increasing the

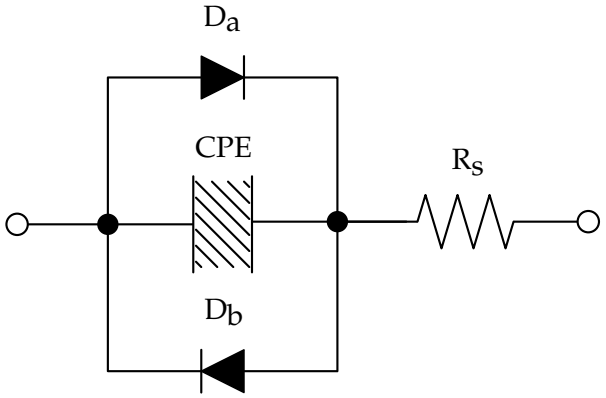

Figure 1.7: Electrical schematic of the electrode-electrolyte interface without memristors (as used throughout this thesis)

resistance in series with a conducting diode has the effect of removing that diodes current path from the circuit, simulating the depletion of reactants for the modelled reaction.

Memristors were removed from the model used in this thesis as they added complexity that would yield very little value. The diodes are only used to model the *onset* of Faradaic conduction, which is the most relevant parameter of the Faradaic modelling. Once these reactions begin, the electrode overpotential has been pushed too far and there is little to be gained from knowing how far the reaction can be run until the reactants have been depleted. In an implanted setting it is likely that the electrolyte will circulate throughout the body, bringing new reactants to the electrode's surface over time. Species depletion is likely to be a slow process, dependant on the electrolyte volume and species concentration.

Figure 1.7 shows the actual interface model used throughout the remainder of this thesis. Although it is slightly different to the Scott-Single interface model, the other parameters are unaffected by the removal of these elements. Each of the components of the interface model have now been described. A model of the interface on its own is of little value as there will always be two

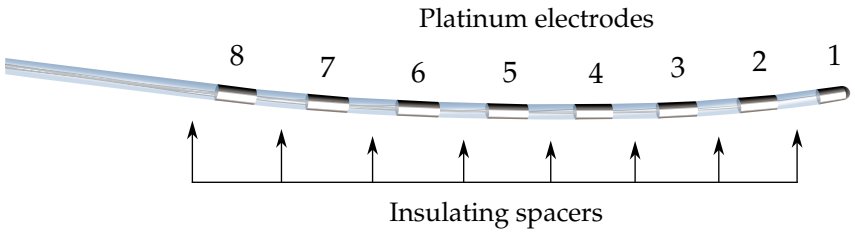

Figure 1.8: St. Jude Medical Octrode. An eight electrode array commonly used in spinal stimulation implants. The electrode numbering shown here will be used throughout this work.

interface models and those models will be separated by the electrolyte itself.

1.1.2 Inter-electrode resistivity

Modelling the resistance between two electrodes in a fixed geometry situation is simply a matter of inserting an appropriately sized resistor between the two interfaces. The resistance is dependant on the electrolyte's conductivity, the combined surface area of the two electrodes and the distance between them. Modelling an electrode array, such as the St. Jude Medical - Octrode, is more complex as it requires a resistor network to describe the inter-electrode resistances. An illustration of an Octrode is presented as fig. 1.8.

Scott and Single create resistor network for modelling the electrolyte conductivity based on the geometry of the electrodes and the resistivity of the electrolyte. By sectioning the surrounding liquid into cylindrical volumes they calculate the equivalent resistance between those volumes both radial and longitudinal directions. The radaii of the volumes double at each layer which correspond to a fixed radial resistance between each layer. There are two different radial resistances, one for the rings expanding from the insulating spacers, and one for those expanding from the electrode cylinders. The two alternate due to each electrode being separated by an

insulating spacer. The longitudinal resistances quarter in size with each ring layer and after the last radial resistor each node it shorted together. The full mesh for the eight electrode array is five layers deep with three rows of padding at each terminating end, totalling two hundred and five resistors in total. Figure 1.9 shows the resistor network schematic. Further details of how the mesh geometry and resistor values were calculated can be found in [6].

The parameters that describe the resistor mesh are:

- R_{eri} - The initial resistance placed radially from an electrode.
- R_{sri} - The initial resistance placed radially from a spacer.
- R_{li} - The longitudinal resistance.
- Depth - Number of layers between the electrode/spacer and the common end node in the ladder
- Padding - Number of spacer layers to be added to the before the first electrode and after the last electrode in the network.

1.2 Electrolyte: Phosphate Buffered Saline

The model has been fitted to phosphate buffered saline (PBS) because it is was closest representation of human spinal fluid known at the time. Engineers at Saluda used a concentration one-tenth that of a standard solution of PBS as a test solution for their spinal implants as they believed it to be a good match. I was not understood how well the one-tenth concentration matched spinal fluid electrically, which is one of the first research questions I set out to answer. The ingredients used to make the stock standard PBS

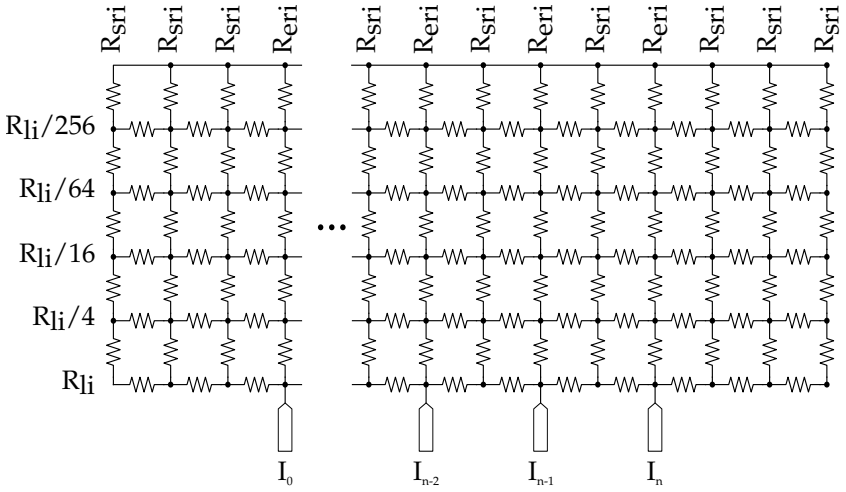

Figure 1.9: Resistor mesh used to model the electrical resistance between interface pairs. R_{li} is longitudinal resistance, R_{sri} and R_{eri} is the radial resistance for the spacers and electrodes respectively, and I is an interface.

Ingredient	Quantity	Unit
H_2O	1000	ml
NaCl	8.00	g
KCl	0.20	g
Na_2HPO_4	1.44	g
KH_2PO_4	0.24	g

Table 1.1: Ingredients used to produce one litre of stock solution of phosphate buffered saline.

concentration solution are given in table 1.1 and the procedure for creating the full strength stock are as follows.

1. Weigh out day ingredients and combine in stock bottle.
2. 800 ml of distilled water is added to bottle and solution is stirred until all solids have dissolved.
3. pH is measured and adjusted to 7.4 by addition of HCL.
4. The stock solution was mixed up to the target volume of 1000 ml.

Six bottles of ranging in concentration from full strength (1.0X) to one-fortieth (0.025X) were then made from the stock solution. Table 1.2 shows

Stock (ml)	Water (ml)	Final Concentration
700.0	0.0	1.00X
350.0	350.0	0.50X
175.0	525.0	0.25X
70.0	630.0	0.10X
35.0	665.0	0.05X
17.5	682.5	0.025X

Table 1.2: Final dilutions of stock to create six 700 ml solutions ranging from 0.025X to 1X standard PBS concentration.

the volumetric dilution used to create the six concentrations of PBS that are then used to fit the model parameters to.

1.3 Methods Of Parameter Extraction

The model has a number of parameters that are used to set the behaviour of each of the components. Finding suitable values for each of the parameters is critical in ensuring that the final model offers a good representation of the electrode-electrolyte system. The trick to finding suitable parameter values lies in selecting useful measurements of each part of the model, usually by isolating the measurement as much as possible from other model elements. The following sections describe the measurements used to determine parameters used in the final model. Ideally each element in the model would be measured separately, but in some cases it is not possible to totally isolate two areas. Scott and Single found a set of parameters that described the Octrode in a one-tenth concentration solution of phosphate buffered saline (PBS). In this section I create six different solutions of PBS ranging in concentration from 1.0x to 0.025x the concentration of a standard PBS solution. I extend the Scott-Single model to work over a range of concentrations of PBS by adding another parameter to the model - PBS concentration.

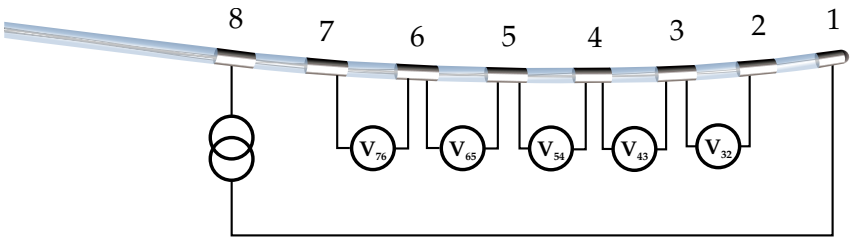

Figure 1.10: Measurement schematic of trans-impedance measurements where electrodes eight and one are driven and the remainder are used in voltage differential measurements.

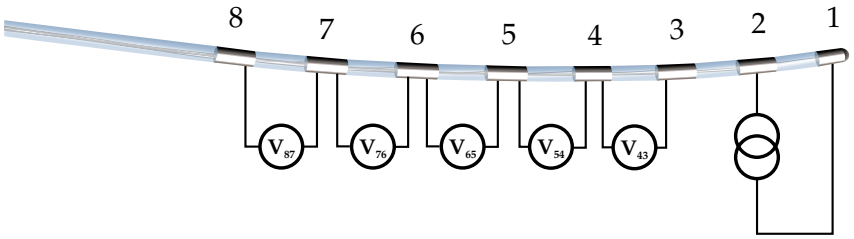

Figure 1.11: Measurement schematic of trans-impedance measurements where electrodes two and one are driven and the remainder are used in voltage differential measurements.

1.3.1 Resistivity

In order to find the parameters of any elements within the electrode-electrolyte interface it is first necessary to find the inter-electrode resistances. This is because elements of the model can not be measured in isolation since the resistivity of the electrolyte solution will always present itself between a measurement apparatus and the element of interest. I start by determining the resistances used in the resistor mesh using the same method as was used by Scott and Single [6]. Once those resistances are accounted for, the behaviour of components in the interface can be calculated from measurements that included those inter-electrode resistances by subtraction.

Scott and Single measure trans-impedance between pairs of electrodes in two different configurations where a defined AC current is driven between a pair of electrodes. Data from these measurements is tabulated so each

Parameter	Determined from:
R_{eri}	optimised fit via SPICE simulation
R_{sri}	optimised fit via SPICE simulation
R_{li}	optimised fit via SPICE simulation
Padding	previous value of 3 rows used (from Scott & Single)
Depth	previous value of 5 layers used (from Scott & Single)

Table 1.3: Parameters determined by an optimised fit between a simulated mesh and transimpedance measurements.

row contains the AC current forced between the two stimulus electrodes and a voltage measured between a pair of non-driven electrodes. By measuring the voltage across pairs of non-driven electrodes using a suitably high impedance measurement, those measurements will correspond to the voltage difference in the electrolyte. For this method to work it is assumed that the current passing through each non-driven interface is zero, and therefore no voltage is dropped between the electrode's metal and the electrolyte solution at the electrode's surface. This means that voltage differentials can only be measured on the non-driven electrodes. Figures 1.10 and 1.11 show the two measurement configurations used to collect transimpedance data. Those transimpedance results are recreated using a simulated mesh of resistors with fitted values to the three resistor parameters. An optimisation routine can be used to find the three values that create a mesh that matches the measured values as close as possible, as summarised in table 1.3.

1.3.2 Constant phase element and series resistance

By accounting for the value of resistance seen between electrodes it is now possible to probe deeper into the interface model. Calculation of both the CPE and the series resistance (R_S) is made via impedance spectroscopy. It is possible to use the applied frequency to separate the response of the CPE

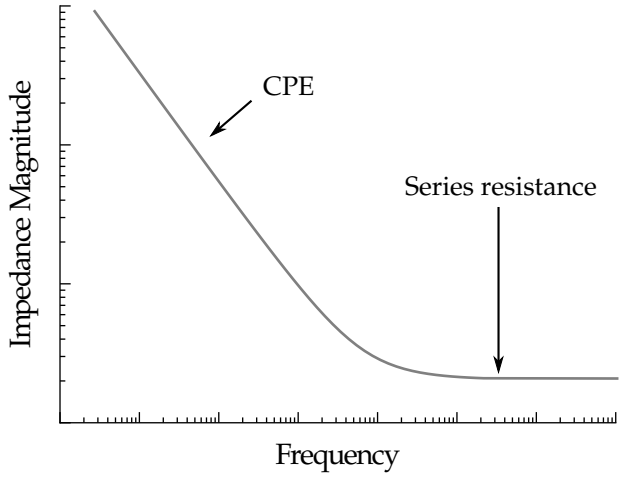

Figure 1.12: Log-log plot of frequency vs impedance magnitude of a single interface and inter-electrode impedance. The response of the CPE and that of the total series resistance is separated in the frequency domain.

from that of the series resistance of a single interface and inter-electrode resistance. The impedance of the CPE dominates below 10 Hz, where its slope and magnitude can be determined. At higher frequencies, greater than 1 kHz, the series resistance of both the interface (R_S) and the previously determined inter-electrode resistance is evident. This separation of responses is illustrated in fig. 1.12. Subtracting the inter-electrode resistance (determined previously) from the resistive element yields just the interface's series resistance (R_S). Parameters for the CPE, such as slope and vertical position, are then read off the low frequency part of the trace where the slope is not disturbed by the resistive part. These parameters are summarised in table 1.4.

1.3.3 Faradaic currents

Measurement of Faradaic current requires pushing the electrode overpotential until reactions at the electrode's surface begin. Electrical currents involved with Faradaic conduction increase exponentially with increasing

Parameter	Determined from:
k	previous value of 3 branches used (from Scott & Single)
m	slope of |Z| vs. frequency response
|Z| @ 1 Hz	impedance magnitude at 1 Hz
R_S	impedance at high frequency (10 kHz) end of the trace

Table 1.4: Parameters determined from impedance spectroscopy measurements of electrode-electrolyte interface.

electrode overpotential. Scott and Single used a triangular voltage stimulus to identify the onset of Faradaic conduction at the interface. The triangular wave is equivalent to a constant ramp-up and ramp-down of voltage placed across the interface. It was mentioned earlier that current flowing into a capacitor is given by: $I(t) = C \times \frac{dV(t)}{dt}$. When $\frac{dV(t)}{dt}$ is a constant, as is the case for any constant ramp-up or ramp-down voltage stimulus, the current becomes a constant. It is assumed that the fractional differentiation of the current equation will still yield a relatively constant current in light of the capacitor being a CPE. By slowly ramping the electrode overpotential up the current should be constant up to a point where it becomes exponential. The voltage corresponding to the point at which the current draw becomes exponential will be used to determine the onset of Faradaic conduction. That point, together with the rate of growth, would then used to fit values for i_0 and n, the diode's saturation current and ideality factor respectively, as summarised in table 1.5. Problems arose with those measurements, which will be discussed in the following section, that show the behaviour of the CPE was less predictable than expected.

Parameter	Description
i_0	optimised fit of threshold voltage to measured curve
n	optimised fit of growth rate to measured curve

Table 1.5: Parameters determined from fitting diode parameters to measured response of Faradaic current.

Chapter 2

Interface Parameters

Details of components in the electrode-electrolyte interface model and methods of determining its parameters have been discussed. The focus now moves to measuring and fitting of the model parameters to the model. Model parameters are determined for a range of concentrations of phosphate buffered saline (PBS), and then for comparison – in a live sheep's spinal cavity. The comparison will tell us whether a one-tenth concentration of PBS is in-fact a good substitute for cerebrospinal fluid (CSF), which it is assumed to be by implant engineers.

2.1 Phosphate Buffered Saline

Scott & Single fitted parameters of their model to a one-tenth concentration (0.1X) of a standard solution of PBS [6]. I measure and fit parameters not only to the one-tenth concentration of PBS but to six concentrations spanning 0.025X to 1X the concentration of a standard saline solution. For the model parameters that change with the concentration of PBS, a fit is made using regression analysis to the concentration. Doing this gives a a model that can be used to predict the impedance response of an electrode array submerged in a wider range of saline solutions.

Concentration
1.00X
0.5X
0.25X
0.1X
0.05X
0.025X

Table 2.1: Six PBS concentrations used to fit model parameters to.

Each of the PBS measurements were made in 1000 ml glass bottles containing 700 ml of PBS solution in each case. Measurements were made in a temperature controlled environment maintaining an ambient temperature of 23° Celsius. All measurements were automated by the use of Python scripts running on a GNU/Linux based workstation. The scripts communicate with the instruments both to configure measurements and collect data. Each measurement set was repeated for each of the six concentrations of PBS used. The six concentrations of PBS that were measured are shown in table 2.1.

2.1.1 Resistor Mesh

With the electrode array immersed in a solution of PBS, a 10 kHz sinusoidal current having an amplitude of 500 µA was passed through the stimulus electrodes using an Agilent 33220A function generator. A current sense resistor was inserted in series with the stimulus electrodes. The differential voltage across a pair of non-stimulating electrodes and the voltage across the current sense resistor was measured using a Tektronix TPS 2024 oscilloscope. Figure 2.1 shows the measurement configuration used when electrodes one and eight are used as the stimulus electrodes. The second configuration has electrodes 8 and 7 as stimulus electrodes and the remaining electrode pairs are used to measure transimpedance voltage differentials.

The results of those measurements, in both configurations, are repre-

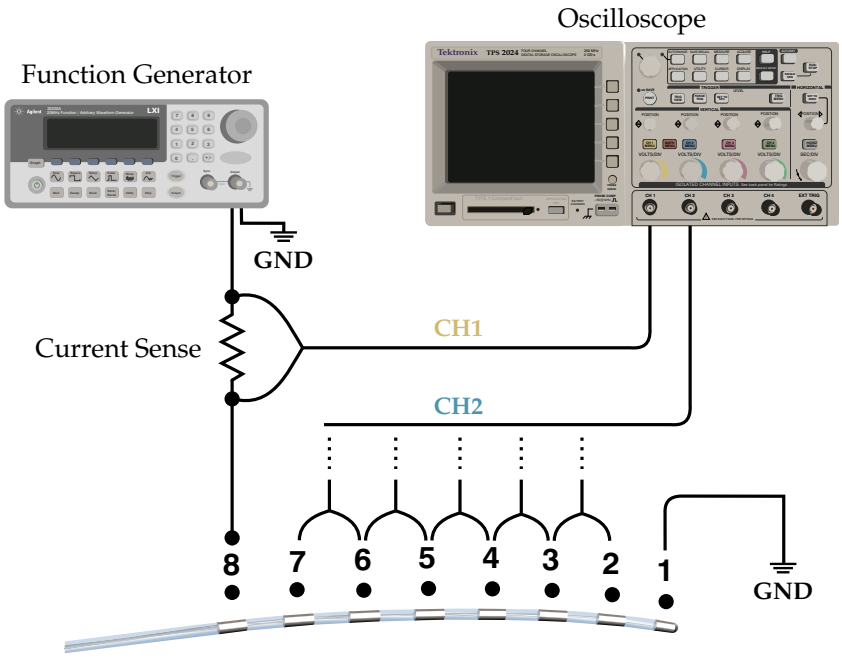

Figure 2.1: Illustration of one of two measurement configurations used to to measure the electrode transimpedances. Each of the electrode pairs were measured one-after-the-other using the shown equipment.

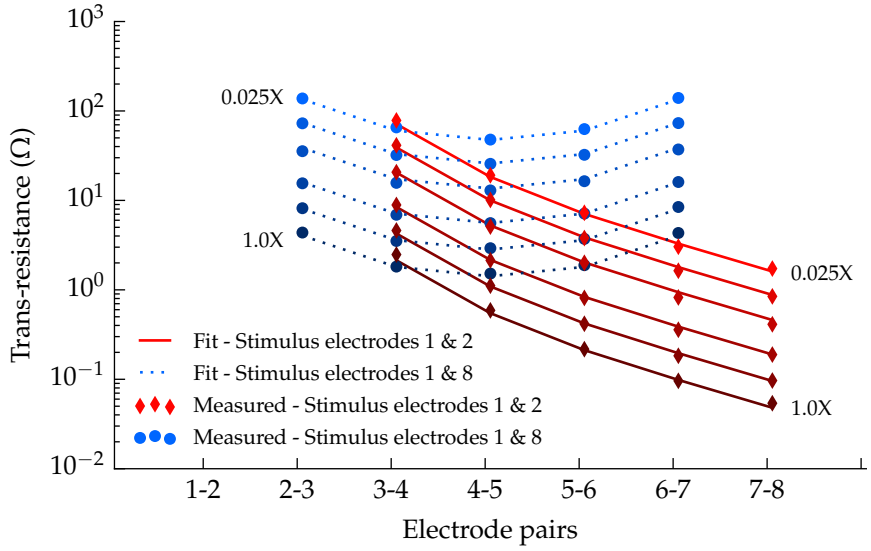

Figure 2.2: Measured and fitted values of trans-impedance for both measurement configurations. Voltage measurements are made between adjacent pairs of electrodes as current is pushed through the stimulus electrodes.

Parameter	Value
R_{eri} (Ω)	$0.407 \ / \ \sigma$
R_{sri} (Ω)	$R_{eri} \cdot 3/4$
R_{li} (Ω)	$3.71 \ / \ \sigma$
Depth (layers)	5
Padding (layers)	3

Table 2.2: Resistor mesh parameters. Electrolyte conductivity (σ) is expressed in units of S/cm.

sented as markers in fig. 2.2. Each point is calculated by taking the voltage differential between a pair of electrodes (V_{diff}) and dividing by the measured stimulus current. The stimulus current was set to be around 500 µA.

The parameter values for R_{eri} and R_{li} were determined using a Python optimisation script for each concentration of PBS. The optimisation script selects candidate values for R_{eri} and R_{li}, simulates the mesh using those values, and then calculates the equivalent trans-impedance values. The error between simulated trans-impedance values and measured values is calculated and the process repeats, selecting different values of R_{eri} and R_{li} to improve the fit. The final values of R_{eri} and R_{li} are those that minimise the error, they are shown in table 2.2. R_{sri} is a dependent variable, so is expressed in terms of R_{eri}, and the remaining parameters have been re-used from the work of Scott & Single. Figure 2.2 shows measurement results for each pair of non-stimulated pair of electrodes along with simulated results using the fitted parameters.

2.1.2 Series Resistance And Constant Phase Element

Measurement of both the CPE and the interface's series resistance is made using impedance spectroscopy methods. The measurement was conducted by passing a sinusoidal current between electrodes two and seven of the

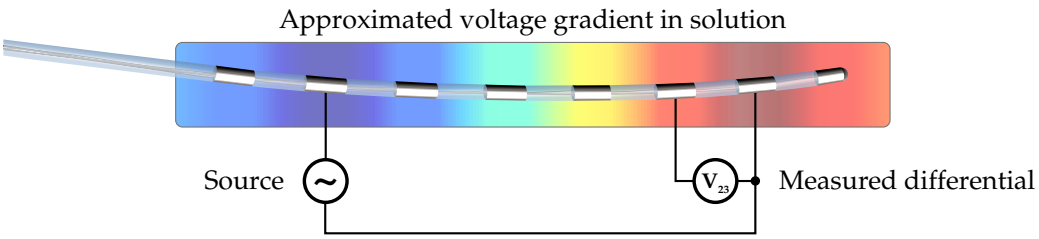

Figure 2.3: Illustrated voltage gradient in electrolyte solution at each electrode's surface when potential is applied across electrodes two and seven. Measurement of electrolyte voltage taken between electrodes 2 and 3.

electrode array. Use of the end electrodes (one and eight) was avoided as a precaution to reduce any end effects. The sinusoidal voltage at the liquid side of the interface is taken as the the voltage that appears at an adjacent electrode (electode three) when a suitably high impedance measurement is made, this is illustrated in fig. 2.3. This measurement relies on the ability to make high impedance voltage measurements to minimise voltage drop across the electrode interface, for which a Tektronix TPS 2024 four channel oscilloscope was used. All four of its channels are floating and have an input resistance of 10 MΩ using 10X probes. An Agilent 33220A Function Generator was used to generate the stimulus waveforms applied between electrodes two and eight. A current sense resistor of 10 kΩ was inserted in series with the waveform generator's output and was measured by the oscilloscope. By measuring the current through electrode two and the voltage across electrodes two's interface, the impedance of the interface is calculated. A diagram showing the measurement setup is shown as fig. 2.4. For each of the six solutions, twenty frequencies (log-spaced) were sampled between 50 mHz and 10 kHz for the impedance measurements. At each frequency the stimulus waveform amplitude was re-adjusted to be 300 mV-peak as the interface's impedance changed. Figures 2.5 and 2.6 show the calculated impedance magnitude and phase from measurements as markers

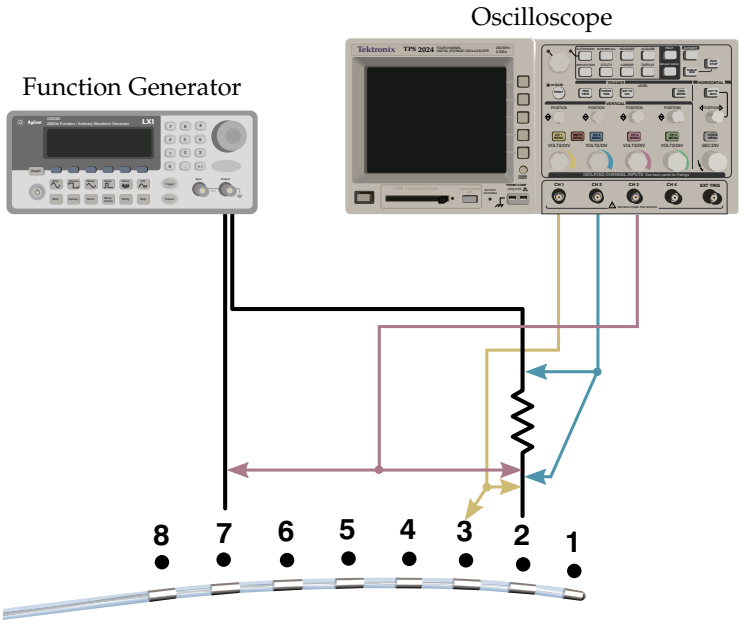

Figure 2.4: Diagram showing the measurement configuration used to measure the CPE response and interface series resistance.

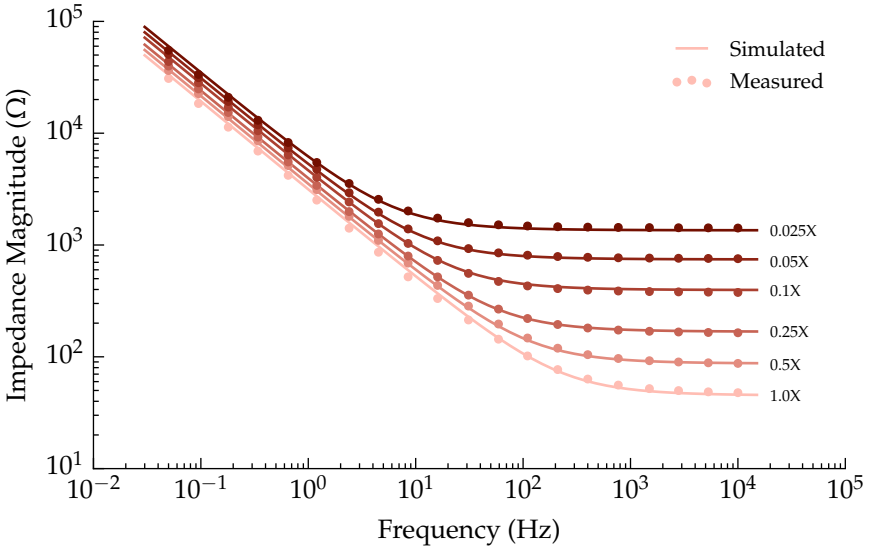

Figure 2.5: Impedance magnitude of both the measured interface response and the fitted response at each of the six concentrations of PBS.

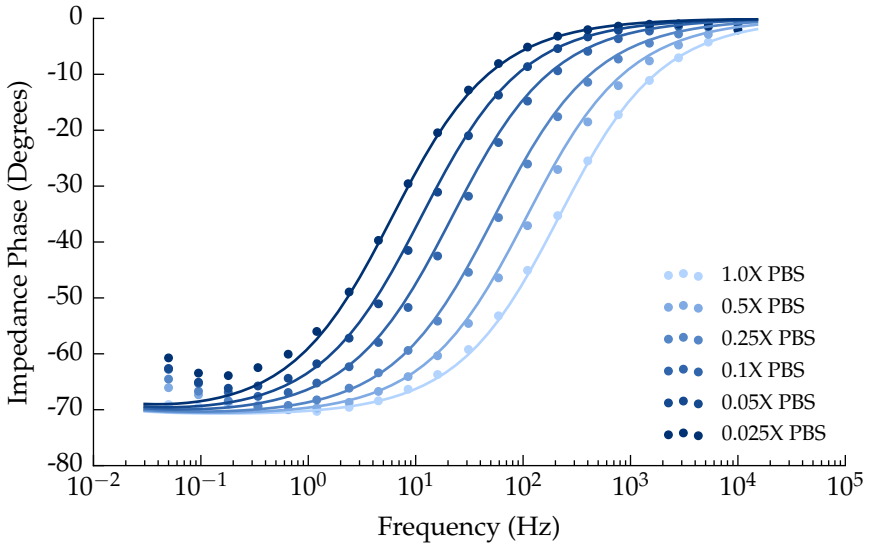

Figure 2.6: Impedance phase of both the measured interface response and the fitted response at each of the six concentrations of PBS.

and simulation results of the fitted parameters as traces. Figure 2.7 shows the SPICE model used to simulate parameter values for the CPE and R_s. Final values were found by minimising the difference between the simulated and measured responses using the Scipy optimisation library available for Python. For each set of parameter values in the optimisation, the script builds a SPICE circuit using those parameter values, then simulates the circuit, then calculates the interface impedance and compares the values to the measured results. The process is automated and runs until a minimum error between simulated and measured results is found. Once found, the script exits and displays the final values of each parameter. After parameter values are found for each concentration of PBS, another optimisation is made to scale relevant parameters by the concentration. The parameters that are scaled with concentration are the series resistance (R_S) and the CPE's impedance magnitude at 50 mHz. The final fit expresses these parameters as functions dependent on the concentration of PBS. Individual parameter

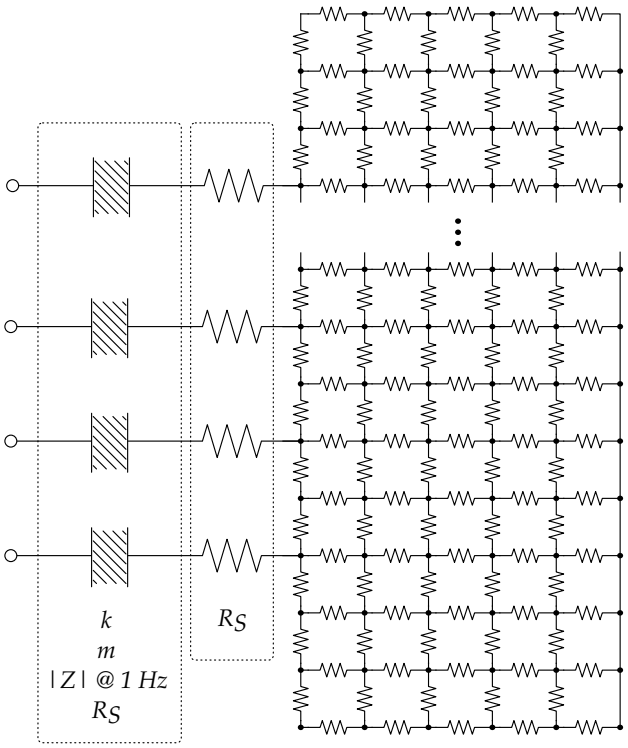

Figure 2.7: The SPICE model schematic used to find optimum values for parameters of the CPE and interface series resistance. Parameters for the resistor mesh are those determined previously.

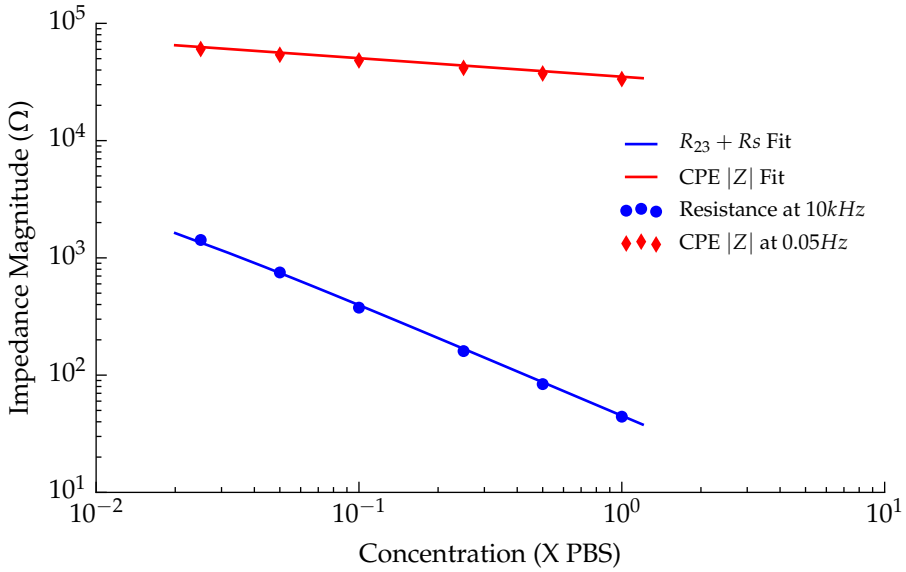

Figure 2.8: Plot showing fitted parameter values for the CPE impedance magnitude at 50 mHz and series resistance at each of the six concentrations of PBS (shown as markers). The solid trace shows the resulting fit between those values as a function of concentration.

Parameter	Value
m	1.34
k	1.773
|Z| @ 1 Hz (Ω)	$3284 \times concentration^{-0.158}$
R_S (Ω)	$13.38 \times concentration^{-0.8397}$

Table 2.3: CPE and R_s parameters. Concentration is relative to the stock solution of phosphate buffered saline.

values for each concentration, along with the resulting fit, is shown in fig. 2.8. Measurements of the CPE's vertical position were made at 50 mHz, as opposed to the parameters defined value at 1 Hz, to avoid any effect from the series resistance interfering with the measured value. As the slope of the CPE is always the same, the value can be easily converted back to the equivalent value at 1 Hz. Measured resistance at high frequency includes the inter-electrode resistance (R_{23}) which has been included in the plot, but will be subtracted to leave only R_S. The final parameters for the CPE and

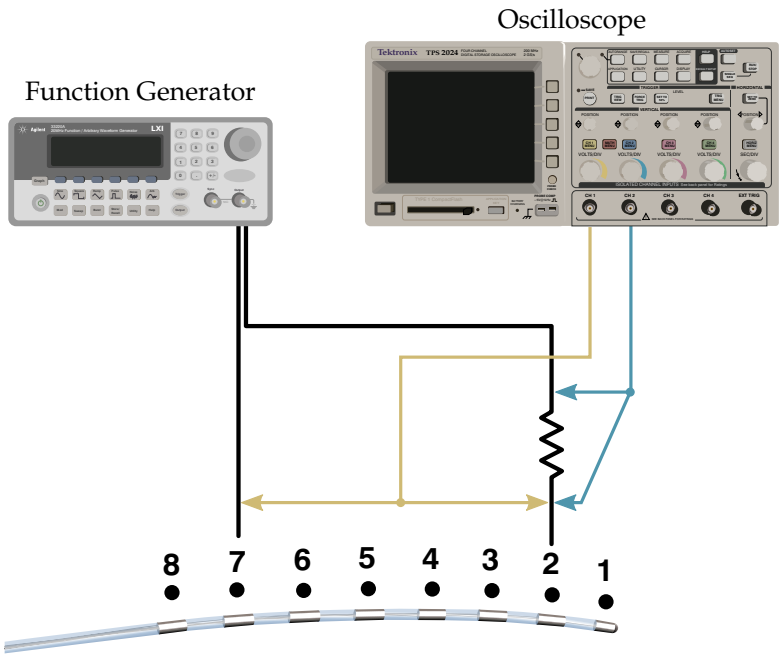

Figure 2.9: Illustration of the cyclic voltammetry measurement configuration used to measure the response of the interface when driven into Faradaic conduction mode.

R_S are given in table 2.3.

2.1.3 Faradaic Current

Using the same oscilloscope and function generator as the previous measurement, the oscilloscope is set to measure voltage between electrodes two and seven and the current through the current sense resistor. The function generator is set to produce a triangle wave stimulus, or linear ramp, also between electrodes two and seven. Electrical current associated with Faradaic reactions rises exponentially after a certain electrode overpotential. The point at which the electrical current draw begins to move exponentially with increasing voltage represents the onset of the associated reaction.

Figure 2.10 shows measured data where the Faradaic response is evident for each concentration. The repeatability of these measurements was low

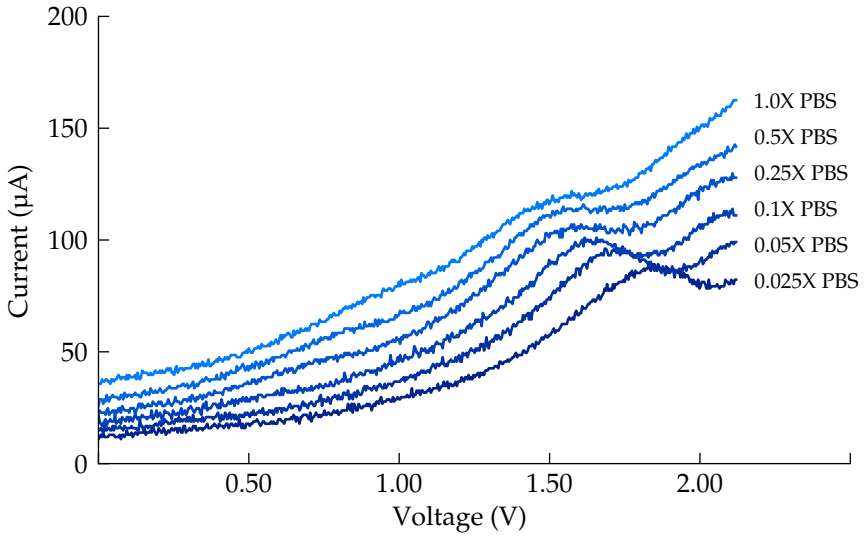

Figure 2.10: Graph showing measured Faradaic response of each concentration of PBS to a linearly increasing voltage between electrodes two and seven.

although care was taken to recreate the same conditions for each run. To try and improve the repeatability the following was tried:

- Maintaining a constant ambient temperature
- Cleaning the electrodes between each measurement using isopropyl alcohol
- Keeping the electrolyte moving at a constant velocity using a motorised stirrer
- Letting the system to settle for periods up to two hours between measurements

These steps reduced variation between measurements, but by no means removed the variation. Sweeping the voltage at $0.12\,\mathrm{V\,s^{-1}}$ was slow enough that results did not appear to be too distorted but fast enough that a measurement run could be completed quickly. Completing measurements quickly

seemed important at the time as it was often the case that an artifact would show up during a measurement run, for what seemed like no apparent reason, and affect the remainder of the experiments. Artifacts were sometimes a peak at a certain voltage, otherwise they would manifest themselves as distortions to the current/voltage trace. A key insight was realising that after the voltage across a pair of electrodes had been pushed into Faradaic region they then began to behave differently, even after being returned to lower stimulus voltages. In fig. 2.10 it is clear that each concentration has a different Faradaic response. This means that when the maximum voltage is applied to each of the solutions that the highest concentration is driven further into its Faradaic region that the rest. That in turn would create an artifact that would appear on the remaining traces (those of lower concentration), that would not have otherwise been there. The issue of artifact and dependence on sweep rate led me to find other ways of measuring Faradaic currents.

2.1.3.1 Step based Faradaic measurements

A revealing measurement came from the use of the Agilent E5270B precision measurement mainframe, the same instrument that was used to measure the streaming potential cells. By increasing the voltage between the electrodes in discrete steps and recording the current over time it became clear that the CPE was having a large effect on measurement results. Figure 2.11 shows three transitions in steps of 0.05 V occurring 64 s apart. The dotted traces show what the result would be if the measurement were taken at that time, i.e. the trace would take the shape of the dotted line of the corresponding delay time. This graph shows the effect the CPE is having on measurement results, as well as the duration of time necessary for the transient response

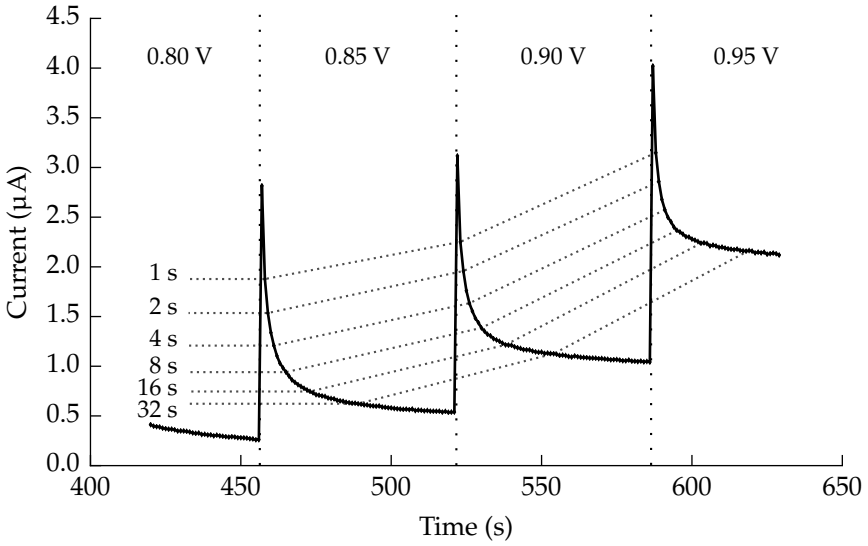

Figure 2.11: Graph showing measured response of two interfaces to a multiple step responses. Vertical dotted lines indicate when in time the step occurred. Dotted traces show points in time after each response. Measurements are between electrodes two and seven on the Octrode submerged in 1X PBS.

to settle.

Subsequent measurements of CPE settling time show that a delay of 64 s between steps is adequate to allow the CPE voltage to settle. These measurements are shown as fig. 2.12, with the 64 s window highlighted in grey. It is interesting to note from these measurements that the capacitance appears to be a function of the applied overpotential, with lower potentials resulting in larger capacitance.

Figure 2.13 shows measurements of four concentrations of PBS overliad on top of one another. This graph reveals that not only does the capacitance vary with applied voltage, as was shown in fig. 2.12, but also with concentration of PBS. A consequence of this is that not waiting long enough to sample the current gives the impression that a higher concentration of PBS results in larger Faradaic currents. This is shown by the dotted trace that is sampled 10 s after each step, which I would argue is somewhat representative of

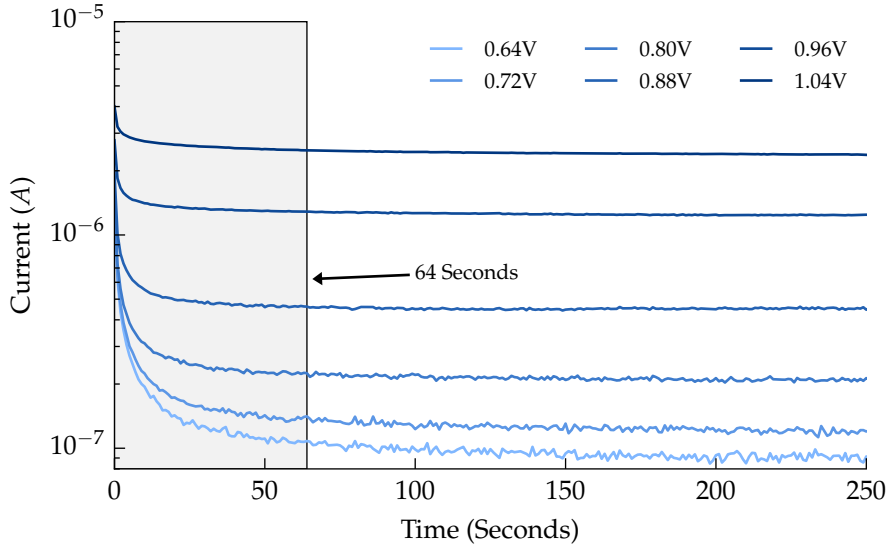

Figure 2.12: Graph showing CPE discharge curve after a step transition between each of voltage trace in increasing order. Measurements are between electrodes two and seven on the Octrode submerged in 1X PBS. A delay of 10 000 seconds elapsed between each step.

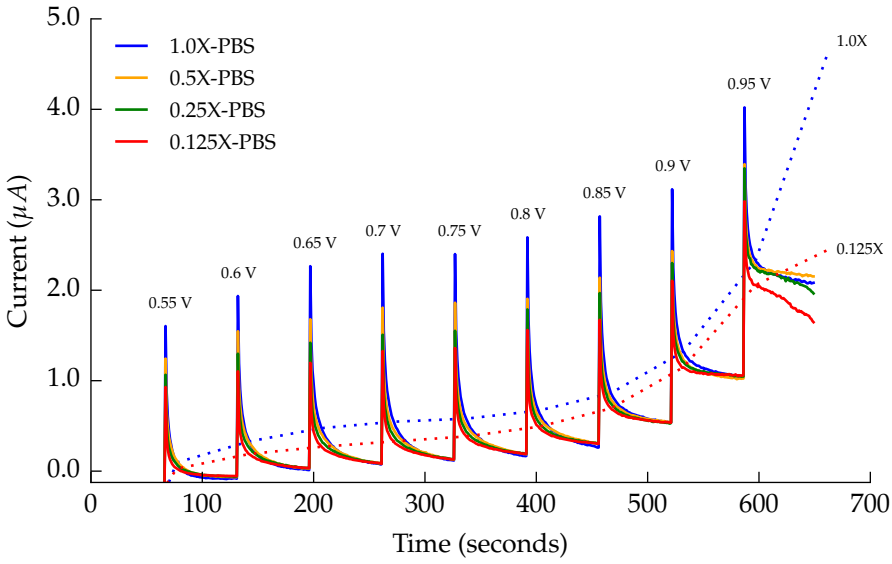

Figure 2.13: Graph showing measurements of four concentrations of PBS as each is stepped from 0.55 V to 0.95 V. Measurements are between electrodes two and seven on the Octrode. A delay of 64 seconds elapsed between each step. Dotted traces connect current measurements taken 10 s after each step.

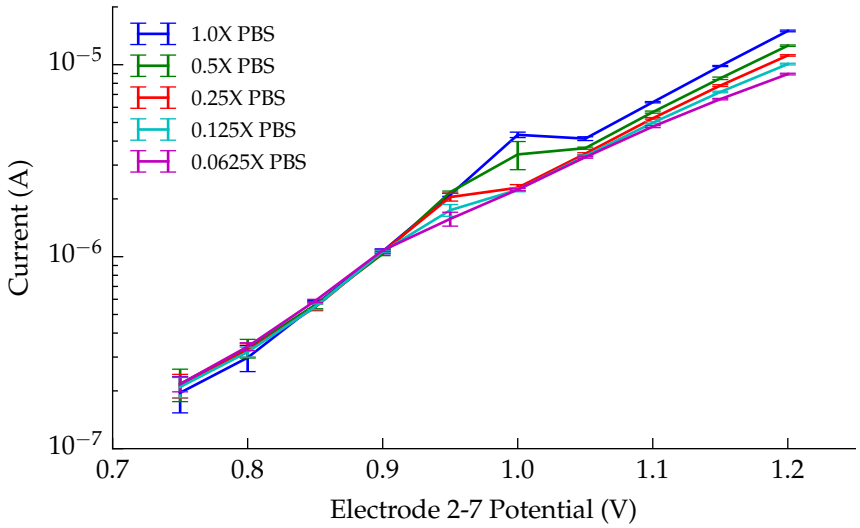

Figure 2.14: Graph showing the electrical current draw associated with Faradaic reactions versus applied electrode overpotential. Measurements used the stepped method with a wait time of 64 s between transitions. Vertical bars mark the standard deviation of the final fourty measurements before the following step.

cyclic voltammetry measurements. Importantly – the settled current draw for each concentration is approximately the same. Any separation between concentrations at the sixty-four second mark for each step appear to be completely random.

2.1.3.2 Successful measurement of the Faradaic currents

Figure 2.14 shows the collected measurements of the electrical current due to Faradaic reactions using the stepped measurement method. Spread in the measurements at low voltages is due to noise in the measurement samples. There are three important observations that can be made from this graph:

1. The effect saline concentration below 0.9 V has little to no significance on the Faradaic current draw.

2. Saline concentration is directly related to Faradaic current draw above

1.05 V.

3. Between 0.9 V and 1.05 V each trace transitions to a mode of saline concentration dependence in reverse order of saline concentration.

2.1.4 Final Model

2.2 Biological parameter measurements

2.2.1 Resistor Mesh

2.2.2 Series Resistance And Constant Phase Element

2.2.3 Faradaic Current

2.2.4 Final Model

Chapter 3

Recipes For Fluid Mimicry

Utilising the measurement methods used previously, I search for a liquid that better replicates a biological impedance. This work is of benefit to engineers of medical implant devices. Having the ability to formulate a solution that mimics the electrical conditions inside a living being greatly simplifies testing.

It was discovered through collaboration with Saluda Medical, developers of stimulator implants, that a solution of one-tenth the standard solution of phosphate buffered saline is used as a test fluid. This solution was the best substitute for a living spine that the engineers had. It was held in large buckets in the laboratories for use whenever a quick test needed to be carried out. Electrodes are submerged into these buckets in order to recreate the electrical conditions inside a human spine.

This was not the only way to simulate the impedance conditions inside a person. As presented in section 2.2, the use of anaesthetised sheep were also used. A sheep's spine has roughly the same dimensions as a humans so it represents a sensible choice in terms of geometry. However, the resources involved with conducting a live sheep trial were high; requiring use of a hospital operating theatre, surgeon veterinarian, and equipment.

Engineers at Saluda had no way of knowing how well those baths of saline represented a sheep's spine. It was shown in section 2.2 that the match between the two was weak. With that knowledge, and the measurement techniques developed thus far, we now ask if it is possible to create a better match. Such a match would reduce the number of surgical operations the test engineers might need to conduct, saving resources.

3.1 Measurements

This work is a very recent addition to the previous work at the time of writing. The measurements were not conducted in a laboratory environment, so it is expected that some inaccuracies will exist. These inaccuracies will be related to:

1. a lack of temperature control, meaning temperatures fluctuated between 18 and 26 degrees;
2. use of consumer grade scales, jeweller's scales for under 5 grams and kitchen above;
3. use of consumer grade ingredients and distilled water.

The measurement equipment used to conduct the measurements were the same as those used in the lab.

3.1.1 Configuration

The function generator, Agilent 33220A, and oscilloscope, Tektronix TPS 2024, are connected to the electrode array, St. Jude Medical - Octrode, as is shown in fig. 3.1. A 10 kΩ resistor was used to measure the current driven between electrodes eight and three. It had a measured resistance of 9.990 kΩ, as measured with a Fluke Digital Multimeter.

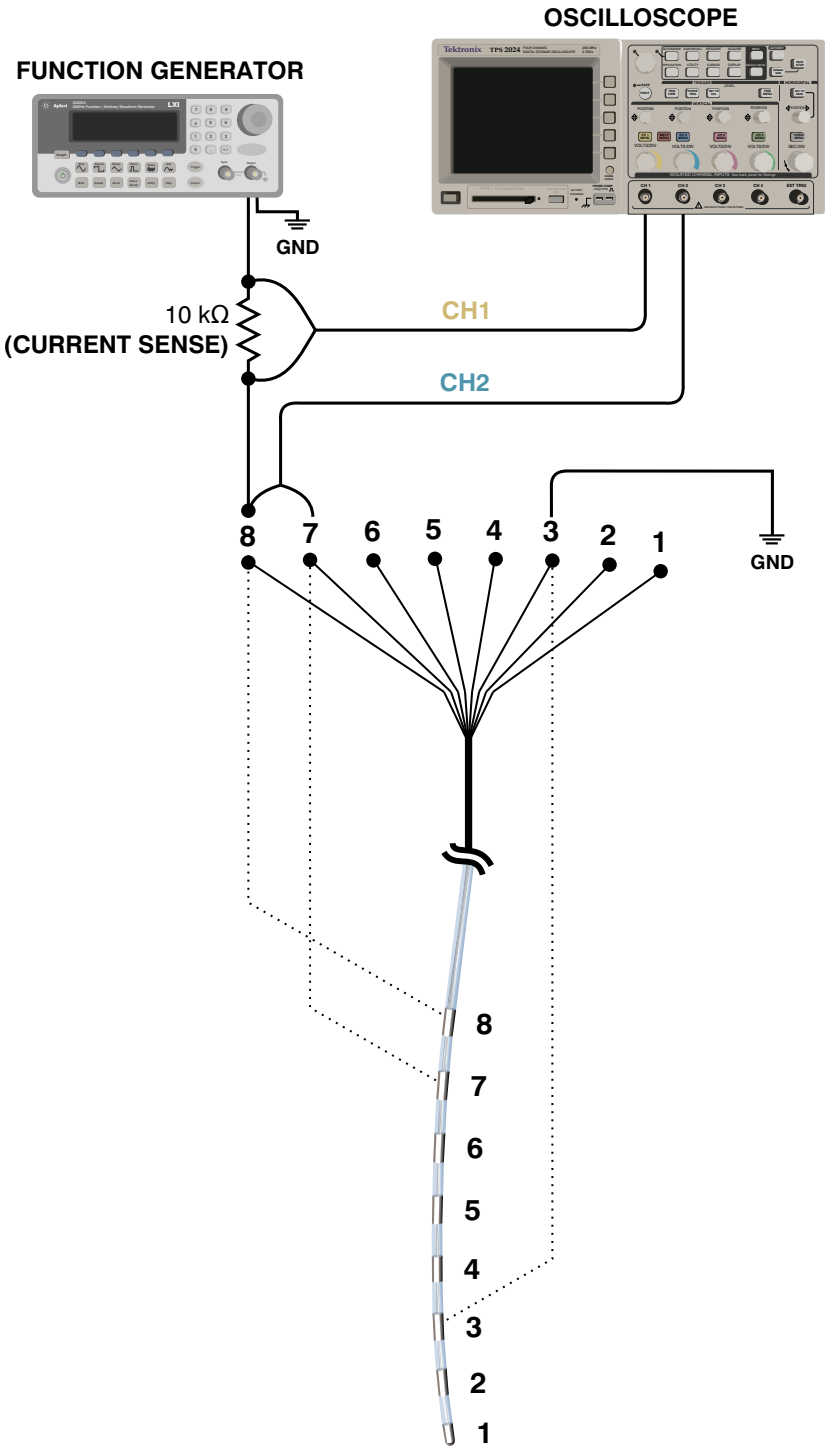

Figure 3.1: Diagram showing the measurement configuration used to measure the CPE response and resistivity of mixed solutions

3.1.2 Procedure

Each measurement run begin at the upper end of the frequency spectrum and proceeded towards the low frequency endpoint. Starting with the higher frequencies offers a chance to confirm correct measurement set-up early in the measurement. A sample at the lowest frequency can take over a minute to acquire, where the higher frequencies drop to under a second. The same frequencies were chosen that were used to measure the situation in live sheep. This allows easy comparison between the sheep data and the impedance of mixed solutions.

Measurements were completely automated via a Linux based computer running Python scripts. These scripts controlled the output settings of the waveform generator and acquired the resulting waveforms from the oscilloscope. The scripts had the ability to set the horizontal and vertical scales on the oscilloscope channels in order to ensure appropriate scales were used. These scripts were written by myself and have been made freely available through my github account (https://github.com/MarkHedleyJones/pyLabInstruments)

The measurement procedure followed by the script is shown as a simplified flowchart in fig. 3.2. The programme steps through each of the required frequencies, making sure the target voltage is developed across electrodes seven and eight, calculating the interface impedance.

The target voltage across the interface is 20 mV. This voltage was previously determined as a safe stimulus voltage in that it does not trigger Faradaic reactions at the electrode's surface. Because the impedance of the interface changes with frequency, it is necessary to alter the output amplitude to keep the voltage across electrode seven and eight consistent.

This measurement configuration differs from the three channel method

```
frequencies = [
 40000,
 16000,
 6700,
 2700,
 1100,
 450,
 190,
 76,
 31,
 13,
 5.1,
 2.1,
 0.86,
 0.35]
```

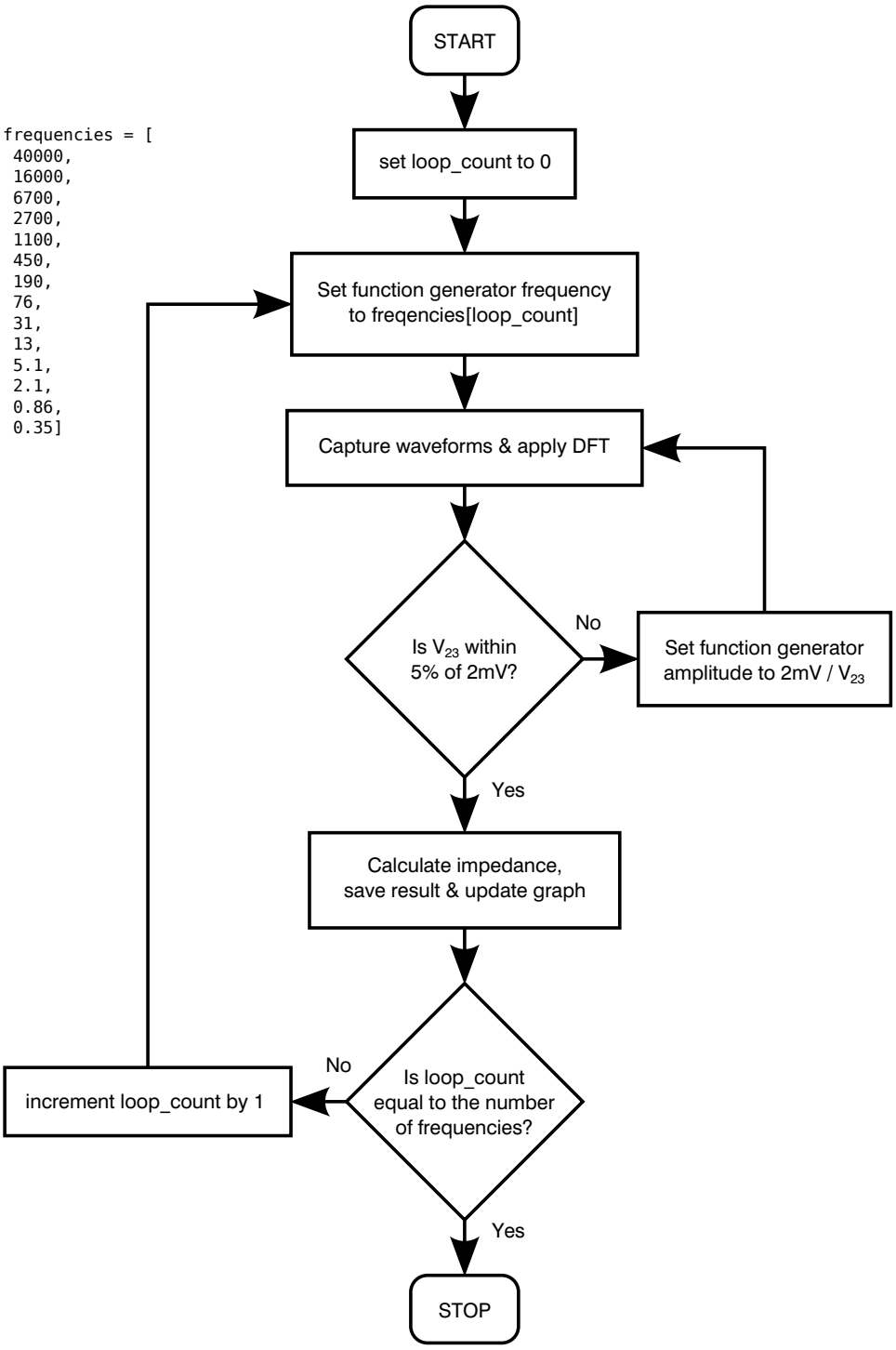

Figure 3.2: Diagram showing the execution of the measurement script

used in earlier measurements. Those used channel three of the oscilloscope to watch the voltage developed between electrodes three and eight.

3.1.3 Ingredients Tried

To determine how certain additives affect the impedance of the interface, a wide range of ingredients were mixed and tested. They were used in a semi-random order, chosen to maximise the usage of the quantity of distilled water available at the time.

- Glycerol
- Methylated Spirits
- Sodium Carbonate
- Sodium Bicarbonate
- Table-salt (non-iodised)
- Gelatine
- Citric Acid
- Corn-flour

3.1.4 Results

Water, Corn-flour and Salt

Figures 3.3 to 3.10 show a progression of measurements beginning with distilled water, then adding cornflour, then adding salt, and finally adding a very small amount of extra water.

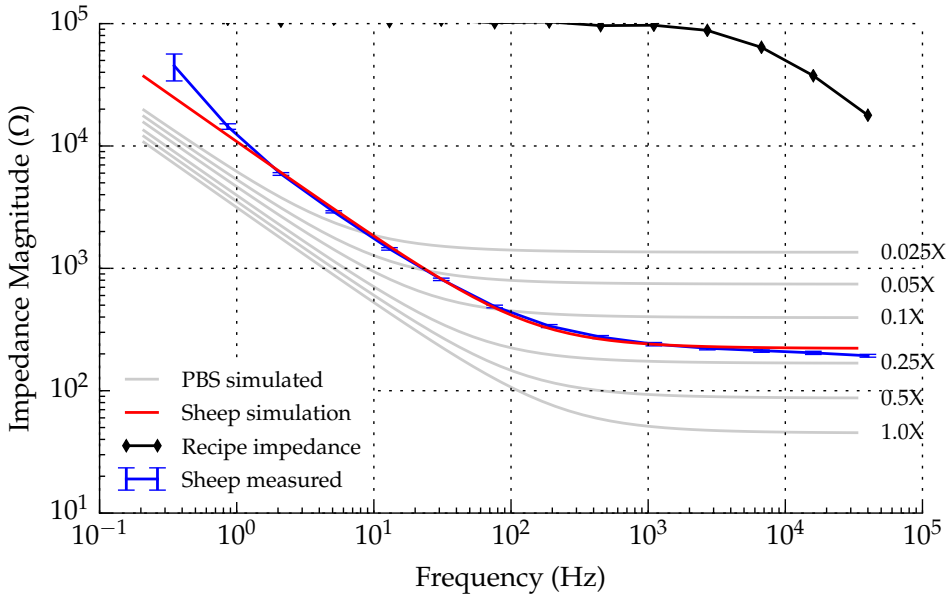

Figure 3.3: Plot of impedance magnitude versus frequency (log-log) for distilled water.

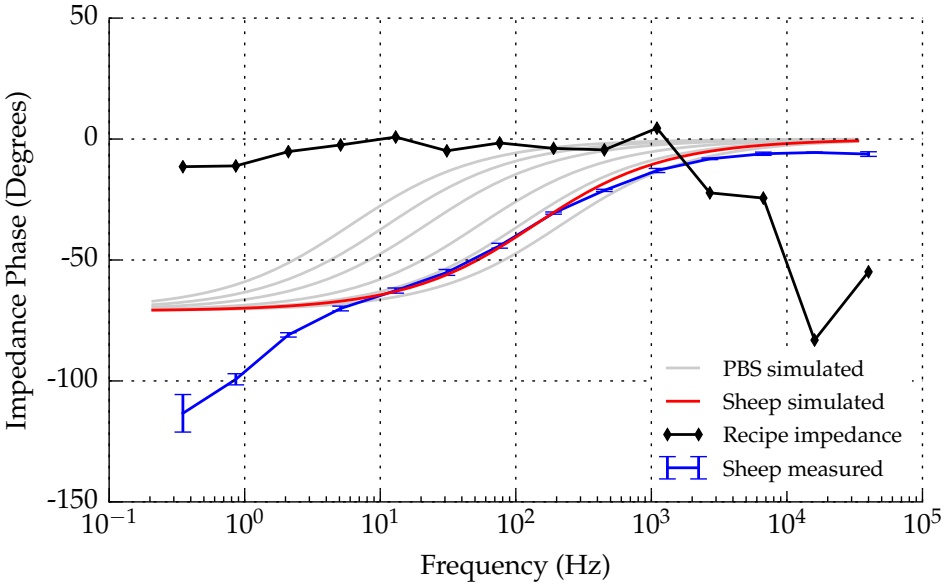

Figure 3.4: Plot of impedance phase versus frequency (log-log) for distilled water.

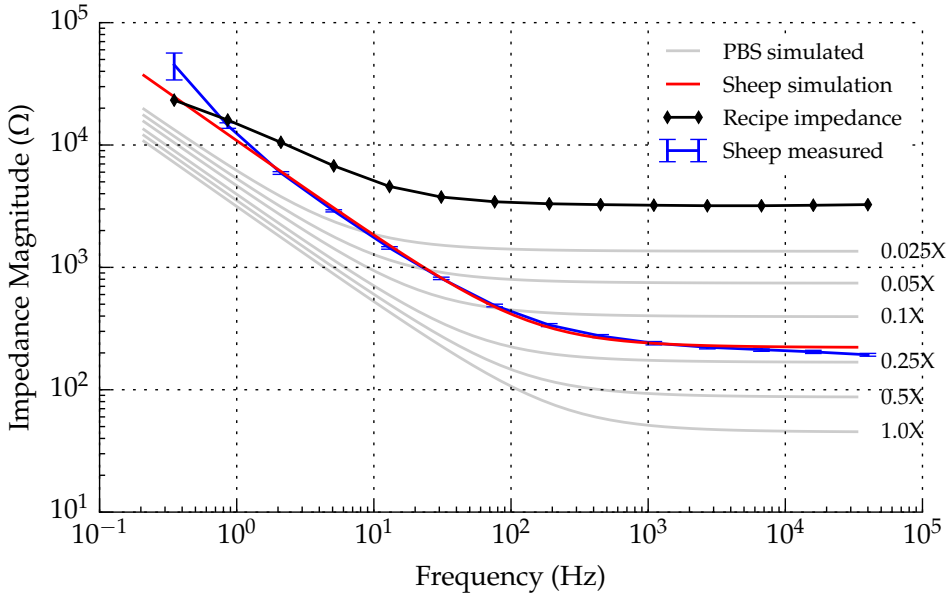

Figure 3.5: Plot of impedance magnitude versus frequency (log-log) for 250 g cornflour mixed with 175 ml distilled water.

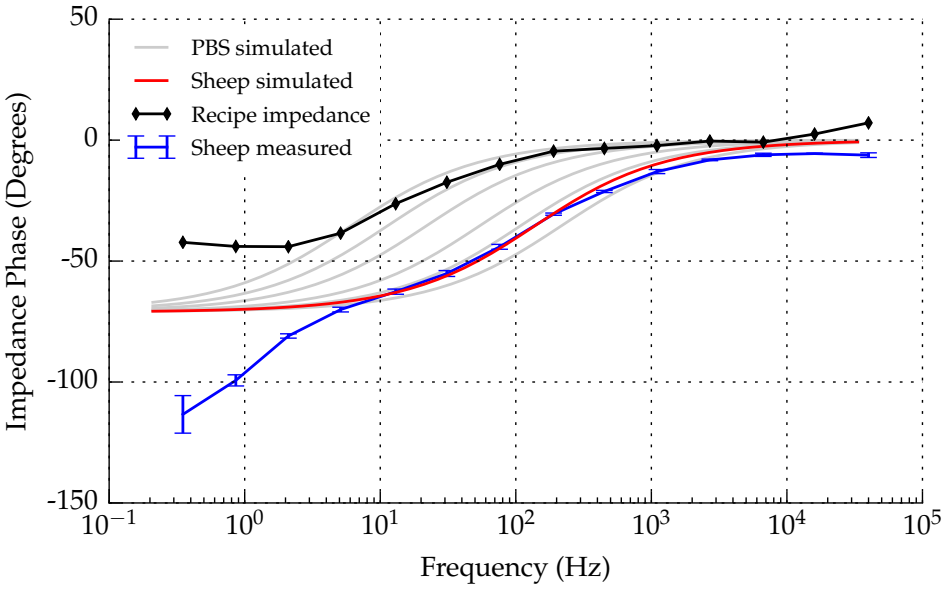

Figure 3.6: Plot of impedance phase versus frequency (log-log) for 250 g cornflour mixed with 175 ml distilled water.

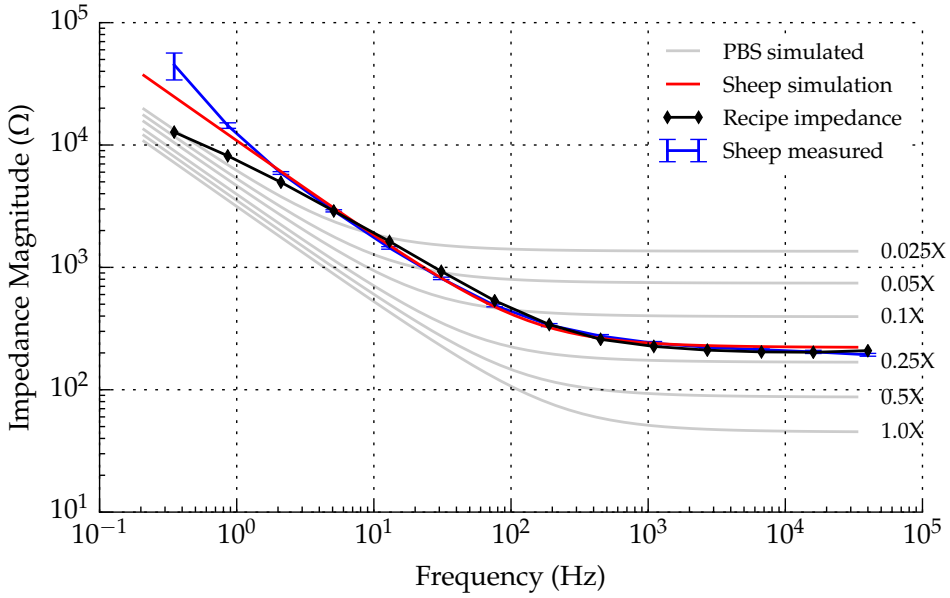

Figure 3.7: Plot of impedance magnitude versus frequency (log-log) for 250 g cornflour mixed with 175 ml distilled water and 1.9 g table-salt.

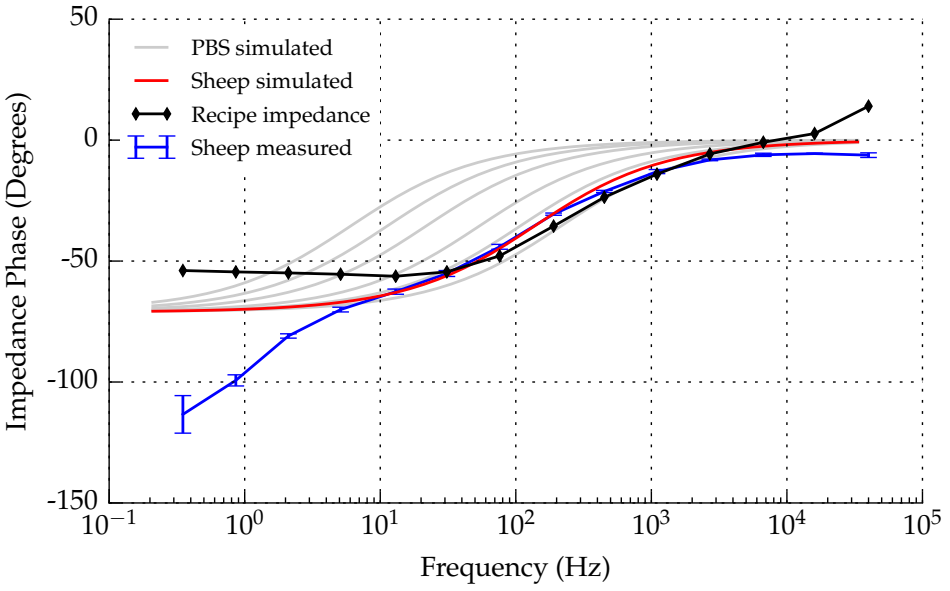

Figure 3.8: Plot of impedance phase versus frequency (log-log) for 250 g cornflour mixed with 175 ml distilled water and 1.9 g table-salt.

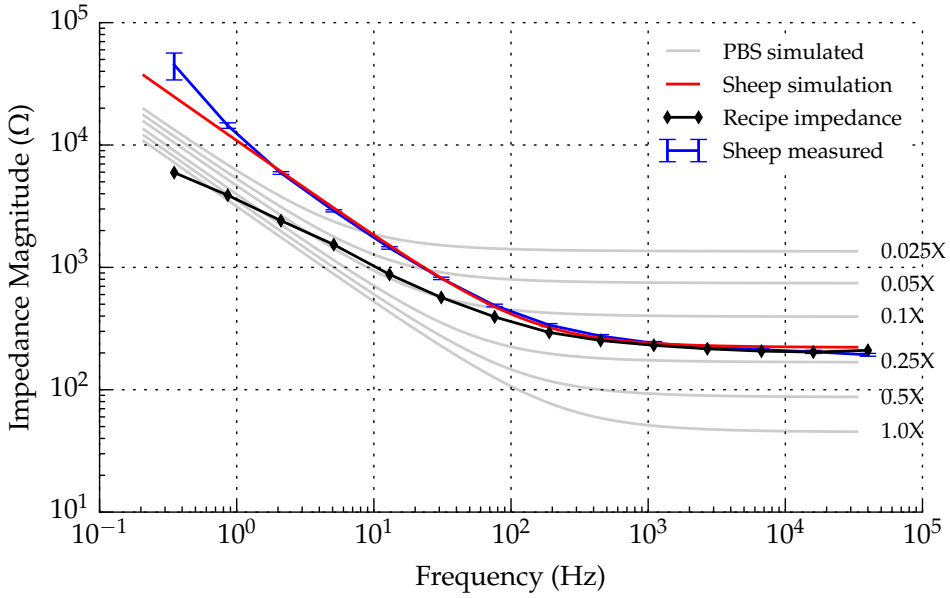

Figure 3.9: Plot of impedance magnitude versus frequency (log-log) for 250 g cornflour mixed with 180 ml distilled water and 1.9 g table-salt.

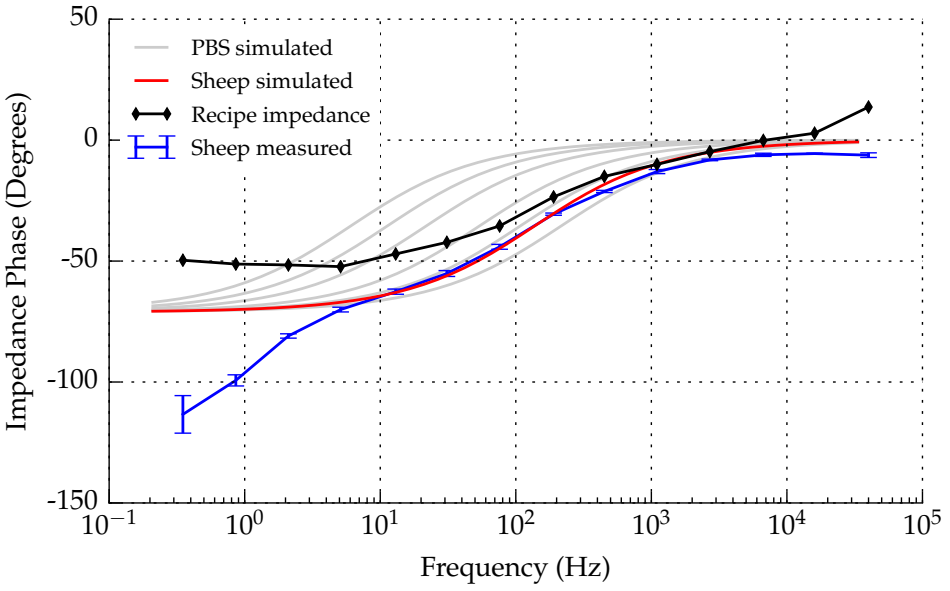

Figure 3.10: Plot of impedance phase versus frequency (log-log) for 250 g cornflour mixed with 180 ml distilled water and 1.9 g table-salt.

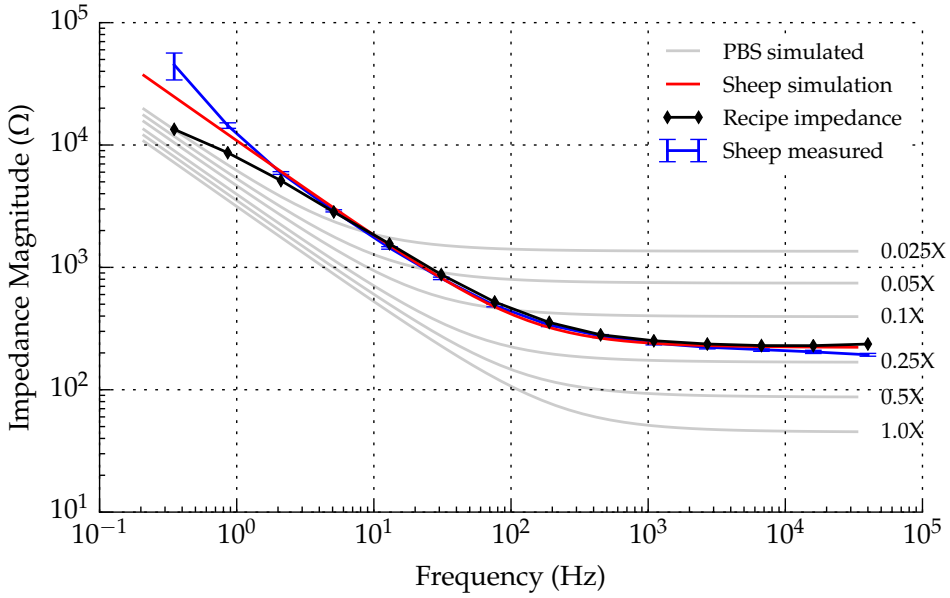

Figure 3.11: Plot of impedance magnitude versus frequency (log-log) for 190 g cornflour mixed with 190 ml distilled water and 0.858 g table-salt.

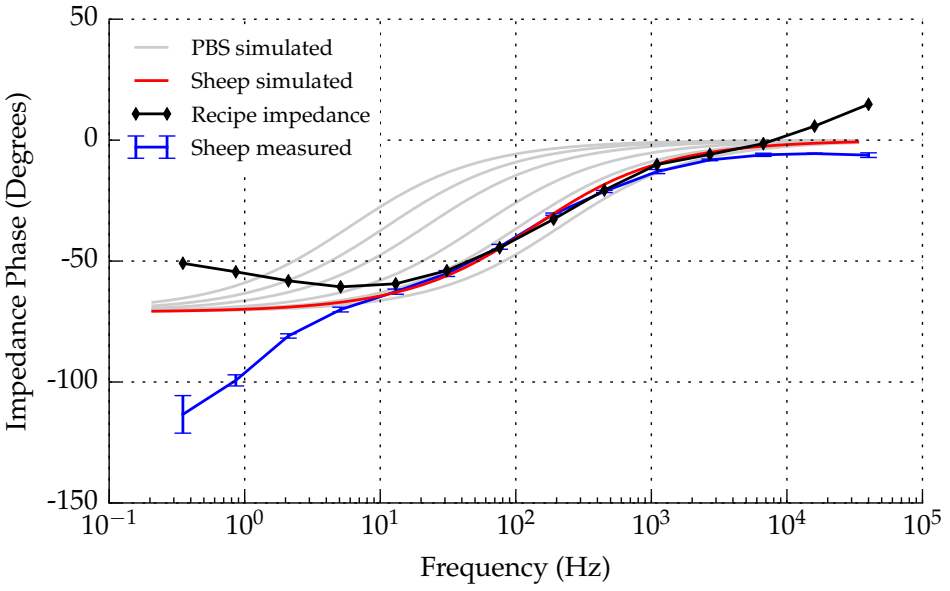

Figure 3.12: Plot of impedance phase versus frequency (log-log) for 190 g cornflour mixed with 190 ml distilled water and 0.858 g table-salt.

Improved Water, Corn-flour, and Salt

Figures 3.11 and 3.12 show the results of mixing the same set of ingredients as the previous measurement set, but with the closest fit to sheep spine obtained.

3.1.5 Discussion

These results show that it is possible to alter the CPE response and the bulk conductivity of the solution independently of one another.

Each of the measurements that contained salt had a tendency to "fall-over" at low frequency. The salt

Notes

The text width of this thesis is 360.0pt.

The text height of this thesis is 595.80026pt.

Bibliography

[1] Shahar Kvatinsky, Keren Talisveyberg, Dmitry Fliter, Avinoam Kolodny, Uri C. Weiser, and Eby G. Friedman. Models of memristors for SPICE simulations. In *2012 IEEE 27th Convention of Electrical and Electronics Engineers in Israel*, pages 1–5. IEEE, November 2012. 1.1.1.4

[2] ET McAdams, A Lackermeier, J.A. McLaughlin, D. Macken, and J. Jossinet. The linear and non-linear electrical properties of the electrode-electrolyte interface. *Biosensors and Bioelectronics*, 10(1-2):67–74, January 1995. 1.1.1.3

[3] Daniel R Merrill, Marom Bikson, and John G R Jefferys. Electrical stimulation of excitable tissue: design of efficacious and safe protocols. *Journal of neuroscience methods*, 141(2):171–98, February 2005. 1.1.1.3

[4] R Morrison. RC Constant-Argument Driving-Point Admittances. *IRE Transactions on Circuit Theory*, 6(3):310–317, 1959. (document), 1.4, 1.1.1.2

[5] Jonathan Scott, Senior Member, and Peter Single. Compact Nonlinear Model of an Implantable Electrode Array for Spinal Cord Stimulation (SCS). *JOURNAL OF BIOMEDICAL ENGINEERING*, pages 1–8, 2013. 1.1, 1.1.1.3

[6] Jonathan Scott and Peter Single. Compact nonlinear model of an implantable electrode array for spinal cord stimulation (SCS). *IEEE Transactions on Biomedical Circuits and Systems*, 8:382–390, 2014. 1.1.2, 1.3.1, 2.1